INSTITUTE OF PHYSICS PUBLISHING JOURNAL OF PHYSICS B: ATOMIC, MOLECULAR AND OPTICAL PHYSICS

J. Phys. B: At. Mol. Opt. Phys. **35** (2002) 2239–2250 PII: S0953-4075(02)32296-X

Hyperspherical adiabatic eigenvalues for zero-range potentials

G Gasaneo[1,2] **and J H Macek**[1,3]

[1] Department of Physics and Astronomy, University of Tennessee, Knoxville, TN 37996-1501, USA
[2] Universidad Nacional del Sur, Bahia Blanca, Buenos Aires, Argentina
[3] Oak Ridge National Laboratory, PO Box 2008, Oak Ridge, TN 37831, USA

Received 31 December 2001, in final form 11 March 2002
Published 8 May 2002
Online at stacks.iop.org/JPhysB/35/2239

Abstract

The scattering length a associated with two-body interactions is the relevant parameter for near threshold processes in cold atom–atom collisions. For this reason zero-range potentials are traditionally used to model collective behaviour of dilute collections of bosons. The model is also used to compute three-body recombination rates, where it gives an a^4 law. In this paper we examine the applicability of the zero-range model to real physical systems. Hyperspherical adiabatic potentials obtained from the zero-range model are compared with published potentials based on realistic two-body interactions. From these comparisons it is possible to determine the regions where the model applies.

1. Introduction

Near threshold phenomena have attracted attention due to the discovery of Bose–Einstein condensation in dilute vapours of alkali atoms [1], loosely bound He_2 and He_3 molecules [2], and three-body recombination in these systems [4–8]. All of these systems are in the dilute matter regime where clustering and similar phenomena occur. Because the collections of atoms are dilute, interactions at large distances play a critical role. Interactions at small distances are important but need not be known precisely to understand the physical processes. The R-matrix method or the multichannel quantum defect theory (MQDT) formalizes this picture by identifying two regions of coordinate space, one a relatively small region where particles interact strongly and a second asymptotic region of infinite extent where the particle wavefunctions are known exactly. The regions are separated by a surface S on which boundary conditions for the asymptotic wavefunction are specified. This picture has been extensively reviewed in the context of atomic physics [9].

The MQDT method has been formally extended to situations where the physical channels involve more than two fragments by employing a surface [9] specified by a constant value of the hyper-radius R. Despite the simplicity of this picture, it has been extensively applied only when there are two fragments in the asymptotic region. The basic problem for applications to

three or more particle channels is that non-trivial interactions occur at distances large compared with the range of potentials and closed form asymptotic wavefunctions that incorporate these interactions are not known. For that reason, the surface must be taken at very large distances thereby losing the features that have made the MQDT method so fruitful when only two-body channels are open.

To develop the MQDT method for three particle channels, it is necessary to have good wavefunctions for three particles in the asymptotic region. Here the interparticle coordinates are much larger than the range r_{0i} of the two-body potentials yet the two-body phase shifts produced by these potentials are non-negligible and must be self-consistently incorporated into three-particle wavefunctions. In effect, we specify the surface S by constant values of the two-particle coordinates $x_i = r_{0i}$, in addition to a constant value of the hyper-radius. Except for calculations of the wavefunctions for helium negative ions in the adiabatic approximation [10], such surfaces have not been widely applied. Zheng and Macek [11] employed a surface with $x_i > a$ to obtain an asymptotic expansion in powers of a/R for the $J = 0$ adiabatic functions for three bosons, where a is the two-body scattering length and J is the total angular momentum. Calculations of the He trimer [2] indicated that the asymptotic expressions of [11] hold only at very large distances.

To obtain good asymptotic representations of three-body wavefunctions we consider expansions in powers of r_{0i}/R rather than a/R. The first term in such an expansion will be independent of r_{0i}. We can therefore take the limit $r_{0i} \to 0$ as long as the limit exists. In the asymptotic region specifically three-body forces are unimportant for neutral atoms and molecules. In fact any such interactions vanish in the limit that $r_{0i} \to 0$, and are not considered in this manuscript. Interactions described by boundary conditions in the limit $x_i \to 0$ are called zero-range potentials (ZRPs) and are defined formally by boundary conditions at the point

$$\frac{1}{x_i \Psi} \frac{\partial (x_i \Psi)}{\partial x_i}\bigg|_{x_i \to r_{0i}} = -\frac{1}{a_i} \tag{1}$$

where a_i is the scattering length for the ith pair. These quantities are assumed known from experiment or from solutions of the two-body Schrödinger equation for the ith pair. The scattering length could be, in general, different. Such potentials have long been used to model physical systems [12]. Here we emphasize a broader aspect of these potentials, namely, they give the asymptotic wavefunctions for particles interacting via short range interactions. When the boundary conditions are energy independent, then the exact theory for these models leads to integral equations which have been solved numerically for several physically interesting species [7]. No analytic representations emerge even when the $r_{0i} \to 0$, although some progress has been made for a special case [13]. In the broader context of asymptotic solutions we do not calculate physical quantities such as bound states, reaction matrices etc, since these depend upon the wavefunction at both small and asymptotic distances. This report focuses on the asymptotic region where only the two-body scattering length plays a decisive role.

To develop asymptotic wavefunctions it is necessary to have a correct formulation of the scattering theory involving fragmentation channels where three or more fragments are present. The hyperspherical adiabatic representation [14] is one such formulation. It maps all reaction theory onto a set of coupled radial equations identical to those for two-particle channels, but which correctly represent the complete system on the circle at infinity [15] as long as the potentials are short range [16]. The theory is particularly well adapted to threshold phenomena [17, 19] and has been employed, for example, to compute bound states of the helium trimer, halo states of nuclei and three-body recombination [5, 20]. In this paper we use the mass-scaled coordinates of figure 1 defined by $\mu R^2 = x_i^2 + y_i^2$ where $x_i = \sqrt{\mu} R \sin \alpha_i$, $y_i = \sqrt{\mu} R \cos \alpha_i$ and μ is an arbitrary parameter [16].

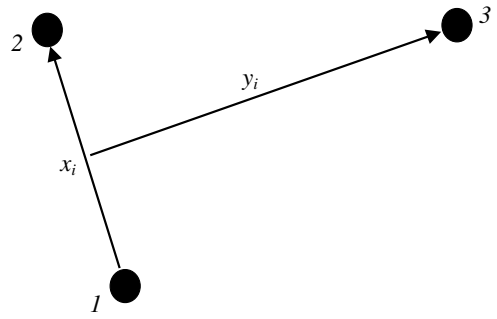

Figure 1. One of the three sets of Jacobi coordinates for three particles from [18].

To use the adiabatic representation it is necessary to compute adiabatic eigenvalues and wavefunctions over a wide range of distances, namely, from the very smallest distances where three particles interact strongly to the asymptotic region where the three particles separate into two- and three-body fragments. Techniques to efficiently compute eigenvalues at small distances are readily available but become inefficient and error prone when employed at large interparticle separations [2,21]. In this case, however, analytic expressions for the asymptotic wavefunctions, energy eigenvalues and coupling matrix elements are known [5, 22] in the ZRP limit for states with $J = 0$ [16, 18]. The methods of [16] also apply to $J \neq 0$. Very recently adiabatic potential curves for a variety of symmetries of the He_3 system have been published [19,23]. The availability of these calculations allows one to identify the region where the asymptotic ZRP representation becomes reliable. In this paper we shall derive expressions for adiabatic potential curves $\varepsilon(R)$ for $J \neq 0$ with ZRPs and shall compare our results with the *ab initio* calculations of [23].

Closed form expressions for $J = 0$ states are given implicitly in [5]. These authors give an expression for the hyper-radius R treated as an eigenvalue in terms of a parameter ν. The function $R(\nu)$ is then inverted to obtain $\nu_n(R)$ where $\nu_n(R)$ are the roots of the equation $R(\nu) = R$. The adiabatic energy eigenvalues $\varepsilon_n(R)$ are then given by

$$\varepsilon_n(R) = \frac{\nu_n(R)^2 - \frac{1}{4}}{2\mu R^2}, \tag{2}$$

where μ is a mass parameter that depends upon the definition of R. In this way one efficiently obtains *all* asymptotic energy eigenvalues $\varepsilon_n(R)$, $n = 1, 2, \ldots, \infty$ from *one* function $R(\nu)$ [24]. This function $R(\nu)$ has been identified as a pseudo-Sturmian eigenvalue and is denoted by $\rho(\nu)$ [13]. For ZRPs it is similar to the logarithmic derivative eigenvalue $B(E)$ of the Fano–Lee R-matrix theory [25]. This becomes clear in our boundary conditions equation (7) below. We do not pursue this connection further but mention it to emphasize that our applications of ZRPs are to be understood in terms of this more general theory. It is also apparent that our adiabatic eigenvalues and those of [5], although they only represent the first term in powers of r_{0i}/R, include all terms in powers of a/R. These expressions thereby supercede the asymptotic expansions of [11]. Expansions in powers of a/R for $J \neq 0$ were given in [16].

2. Hyperspherical adiabatic eigenvalues for ZRPs

The hyperspherical adiabatic theory is a rigorous procedure that reduces the three-body problem to a set of coupled radial equations. Once the centre of mass motion is removed, the three-

body Schrödinger equation reduces to a six-dimensional equation. The hyperspherical coordinates [14] employing a hyper-radius R, two internal angular coordinates and three external angles (generally Euler angles) are a set of six coordinates that efficiently represent fragmentation states. The Schrödinger equation in this coordinate system with a total wavefunction rescaled as $R^{-2}\Psi$ is

$$\left[-\frac{1}{2\mu}\frac{1}{R}\frac{\partial}{\partial R}\left(R\frac{\partial}{\partial R}\right) + H_{\rm ad}(R, \hat{\boldsymbol{R}}) - E\right]\Psi = 0 \tag{3}$$

where

$$H_{\rm ad}(R, \hat{\boldsymbol{R}}) = \frac{\Lambda^2 + 4}{2\mu R^2} + V(R, \hat{\boldsymbol{R}}), \tag{4}$$

μ represents the three-body reduced mass, $H_{\rm ad}(R, \hat{\boldsymbol{R}})$ the adiabatic Hamiltonian, Λ^2 is the grand angular momentum defined in [14] and $V(R, \hat{\boldsymbol{R}})$ is the interaction. The interaction is in general a sum of two-body potentials but could include explicit three-body terms, if appropriate. Since only the two-body scattering length is employed here, we do not include three-body interactions.

The adiabatic representation takes R as a parameter and defines the eigenvalue equation

$$H_{\rm ad}(R, \hat{\boldsymbol{R}})\Phi_n(R; \hat{\boldsymbol{R}}) = \varepsilon_n(R)\Phi_n(R; \hat{\boldsymbol{R}}) \tag{5}$$

for the channel functions $\Phi_n(R; \hat{\boldsymbol{R}})$ and eigenvalues $\varepsilon_n(R)$. This equation, which depends upon all the angles of the problem, gives the potential $\varepsilon_n(R)$ as defined in equation (2) and leads to a set of coupled hyperradial equations derived from equation (3). Further separation of variables is possible since the dependence upon Euler angles can be extracted by taking into account rigid body motion represented by the Wigner functions. In the work reported here, we do not use this separation since the wavefunctions take a sufficiently simple form without using Euler angles explicitly.

As discussed in [13, 30], the ZRP model is correctly defined in three dimensions by boundary conditions. This means that equation (5) becomes

$$[\Lambda^2 - (\nu^2 - 4)]S(\nu, \hat{\boldsymbol{R}}) = 0 \tag{6}$$

with the boundary conditions that the solutions are regular everywhere except at the location of the ZRPs. To locate these ZRPs we use three sets of mass-scaled Jacobi coordinates, see figure 1, introduced by Federov and Jensen [31] which we label $\boldsymbol{x}_i, \boldsymbol{y}_i, i = 1, 2, 3$. For example, $\boldsymbol{x}_1$ labels the coordinate of particle 2 relative to particle 1 and $\boldsymbol{y}_1$ the coordinate of particle 3 relative to the centre of mass of 1 and 2. Other sets are similarly defined. Corresponding to these coordinates we define the hyper-angles α_i as $\tan\alpha_i = x_i/y_i$ and the angular momentum operators $\boldsymbol{l}_{x_i} = -\mathrm{i}\boldsymbol{x}_i \times \boldsymbol{\nabla}_{\boldsymbol{x}_i}$, $\boldsymbol{l}_{y_i} = -\mathrm{i}\boldsymbol{y}_i \times \boldsymbol{\nabla}_{\boldsymbol{y}_i}$ with eigenvalues l_{x_i} and l_{y_i}. The ZRPs are located at $x_i = \alpha_i = 0$, where the function $S(\nu, \hat{\boldsymbol{R}})$ satisfies the boundary conditions

$$\left[\frac{\partial(\sin\alpha_i \cos\alpha_i S(\nu, \hat{\boldsymbol{R}}))}{\partial\alpha_i} + \frac{\rho(\nu)}{a_i}(\sin\alpha_i \cos\alpha_i S(\nu, \hat{\boldsymbol{R}}))\right]_{\alpha_i \to 0} = 0. \tag{7}$$

Here $\rho(\nu)$ represents a pseudo-Sturmian eigenvalue [13] and a_i $(i = 1, 2, 3)$ the s-wave scattering lengths for the ith pair. These conditions are just the standard ZRP boundary conditions written in hyperspherical coordinates with $\rho(\nu)$ substituted for the physical hyperradius R [13]. For three identical bosons, all the masses are equal and a represents the single scattering length.

Equation (6) is solved analytically and its solution is written as a linear combination of products of hypergeometric functions $F[a, b; c; \cos^2\alpha_i]$ [29] and bispherical harmonics

$\mathcal{Y}_{l_{x_i},l_{y_i},J,M}(\hat{\boldsymbol{x}}_i,\hat{\boldsymbol{y}}_i)$, namely

$$S(\nu,\hat{\boldsymbol{R}})=\sum_{i=1}^{3}A_i\phi_i \tag{8}$$

with

$$\phi_i=(\sin\beta_i)^{l_{x_i}}(\cos\beta_i)^{l_{y_i}}F\left[\frac{l_{x_i}+l_{y_i}+2-\nu}{2},\frac{l_{x_i}+l_{y_i}+2+\nu}{2},l_{x_i}+\frac{3}{2},\sin^2\beta_i\right]$$
$$\times\,\mathcal{Y}_{l_{x_i},l_{y_i},J,M}(\hat{\boldsymbol{x}}_i,\hat{\boldsymbol{y}}_i) \tag{9}$$

where $\beta_i=\frac{\pi}{2}-\alpha_i$ [28]. The variable β_i is introduced to connect with the familiar solutions $\sin\nu(\pi-\alpha_i)$ for $l_{x_i}=l_{y_i}=0$. The parity properties of $S(\nu,\hat{\boldsymbol{R}})$ under inversion of the coordinate axes, discussed in [14], are $S(\nu,-\hat{\boldsymbol{R}})=(-1)^{l_{x_i}+l_{y_i}}S(\nu,\hat{\boldsymbol{R}})$.

The Sturmian functions $S(\nu,\hat{\boldsymbol{R}})$ of equation (8) are written in terms of hypergeometric functions that are regular at $\alpha_i=\frac{\pi}{2}$. Consequently, the functions ϕ_i are regular at $\alpha_i=\frac{\pi}{2}$ for all l_{x_i} and ν. They are also regular at $\alpha_i=0$ if ν is an integer and $l_{x_i}>0$. In this case the boundary conditions are trivially satisfied, i.e. equation (7) just reads $0+0=0$ and ϕ_i is a regular hyperspherical harmonic. States with $l_{x_i}>0$ do occur. For example, since the parity of the bispherical harmonic is $(-1)^{l_{x_i}+l_{y_i}}$ and if $l_{x_i}=0$ then $l_{y_i}=J$. It follows that states with parity $\pi=(-1)^{J+1}$ must have $l_{x_i}>0$, and must, in general, be linear combinations of all hyperspherical harmonics with the same λ, J and π but possibly differing in l_{x_i} and l_{y_i}. Such superpositions of differing hyperspherical harmonics, of course, are still hyperspherical harmonics; indeed, any unitary transformation of degenerate harmonics gives a new set of harmonics. The unitary transformation can be chosen to obtain a set with definite symmetry under particle exchange, for example. Only when $l_{x_i}=0$ do we get a non-trivial solution. Then we have

$$\sin\alpha_i\cos\alpha_i\phi_i|_{\alpha_i\to0}\to\frac{\Gamma(l+\frac{3}{2})\Gamma(\frac{1}{2})}{\Gamma(\frac{l+2-\nu}{2})\Gamma(\frac{l+2+\nu}{2})}\mathcal{Y}_{0,l,l,M}(\hat{\boldsymbol{x}}_i,\hat{\boldsymbol{y}}_i), \tag{10}$$

where we have set $l_{y_i}=J=l$. The symbol $\Gamma(z)$ represents the gamma function [29]. For the first term in equation (7) we have the result that

$$\left[\frac{\partial(\sin\alpha_i\cos\alpha_i\phi_i)}{\partial\alpha_i}\right]_{\alpha_i\to0}\to-(2l+1)\frac{\Gamma(l+\frac{1}{2})\Gamma(\frac{1}{2})}{\Gamma(\frac{l+1-\nu}{2})\Gamma(\frac{l+1+\nu}{2})}\mathcal{Y}_{0,l,l,M}(\hat{\boldsymbol{x}}_i,\hat{\boldsymbol{y}}_i). \tag{11}$$

Substituting equations (10) and (11) into (7) we have the main result of this paper, namely

$$\det[-\rho\boldsymbol{I}+\rho_0\boldsymbol{a}-\rho_c\sqrt{\boldsymbol{a}}\boldsymbol{M}\sqrt{\boldsymbol{a}}]=0 \tag{12}$$

where the coefficients $\rho_0(\nu)$ and $\rho_c(\nu)$ are defined by

$$\rho_0(\nu)=2\frac{\Gamma\left(\frac{l+2-\nu}{2}\right)\Gamma\left(\frac{l+2+\nu}{2}\right)}{\Gamma\left(\frac{l+1-\nu}{2}\right)\Gamma\left(\frac{l+1+\nu}{2}\right)} \tag{13}$$

$$\rho_c(\nu)=\left(-\frac{1}{2}\right)^l\frac{\Gamma\left(\frac{l+2-\nu}{2}\right)\Gamma\left(\frac{l+2+\nu}{2}\right)}{\Gamma\left(l+\frac{3}{2}\right)\Gamma\left(\frac{1}{2}\right)}F\left[\frac{l+2-\nu}{2},\frac{l+2+\nu}{2},l+\frac{3}{2},\frac{1}{4}\right], \tag{14}$$

and the matrices $\boldsymbol{I}$, $\boldsymbol{a}$ and $\boldsymbol{M}$ by

$$\boldsymbol{I}=\begin{bmatrix}1&0&0\\0&1&0\\0&0&1\end{bmatrix}\qquad\boldsymbol{a}=\begin{bmatrix}a_1&0&0\\0&a_2&0\\0&0&a_3\end{bmatrix} \tag{15}$$

$$\boldsymbol{M}=\begin{bmatrix}0&1&1\\1&0&1\\1&1&0\end{bmatrix}. \tag{16}$$

Equation (12) defines the eigenvalue $\rho(\nu)$. In the general case where the scattering lengths a_i are different, it defines a cubic equation for $\rho(\nu)$. When two of the a_i are equal, the cubic equation reduces to a quadratic, and when all the scattering lengths are equal, $\rho(\nu)$ is defined by a linear equation. In this last case, equation (12) reduces to

$$\frac{\rho(\nu)}{a} = \rho_0(\nu) - \rho_c(\nu) \tag{17}$$

where a represents the scattering length.

The Sturmian eigenvalue equation (17) and eigenfunction equation (8) with equation (9) represent a complete solution of the pseudo-Sturmian problem. A close connection with the adiabatic eigenvalues and eigenfunction can be established. The function $\rho(\nu)$ is a multivalued complex function and therefore an infinite number of roots $\nu_n(R)$ of the equation $R = \rho(\nu)$ exist. According to equation (2) each root gives rise to the nth adiabatic energy eigenvalue $\varepsilon_n(R)$ [26,27]. If the roots $\nu_n(R)$ are substituted into equation (8) the nth adiabatic eigenfunction, up to a normalization constant, is obtained.

To clarify the connection between the pseudo-Sturmian and the adiabatic eigenvalues we consider the case of $l = 0$. When $l = 0$ equation (17) gives

$$\frac{\rho(\nu)}{a} = \frac{1}{\sin\left(\frac{\pi}{2}\nu\right)}\left[\nu\cos\left(\frac{\pi}{2}\nu\right) - \frac{8}{\sqrt{3}}\sin\left(\frac{\pi}{6}\nu\right)\right]. \tag{18}$$

This is the equation used by Nielsen and Macek [5]. In figure 2(a) we plot $\rho(\nu)$ as a function of ν^2. As can be seen from the figure, $\rho(\nu)$ is a multivalued function; i.e., a given value of ρ corresponds to an infinite number of νs. If the plot of figure 2(a) is rotated and flipped as shown in figure 2(b), then we have a plot of $2\mu\varepsilon(\rho)\rho^2 + \frac{1}{4} = \nu^2$ versus ρ. The multiple branches of the function $\rho(\nu)$ become the different adiabatic eigenvalues. In figure 2 we plot the bound state and three continuum states extracted in this way from equation (18).

Despite the close connection between the Sturmian and the adiabatic functions, it is important to understand their differing roles in physical theory. While the exact solution can be written in terms of the single Sturmian, the adiabatic functions define the physical channels. For large R, $\Phi_n(R; \hat{\boldsymbol{R}})$ becomes the wavefunction for the nth physical channel of the system. The hyperspherical close coupling theory uses these adiabatic channel functions directly, thus computation of the S-matrix and other quantities related to the wavefunction in the asymptotic region follows the conventional coupled channel procedures of MQDT.

The Sturmian functions give a considerably different representation. The function $\rho(\nu)$ is multivalued, thus a whole set of energy eigenvalues is associated with only one Sturmian function [27, 32]. In figure 3 we show the energy curves derived from (2) using (17) with $l = 0$. In addition to the two-body bound state channel, an infinite number of three-body continuum channels appear, all associated with the same Sturmian. Only the lowest three continuum channels are shown. In the Sturmian theory of [13] the channel functions emerge when the exact wavefunction is evaluated at large R using asymptotic methods. Then one finds that the asymptotic solutions correspond to $\rho(\nu) = R$ which identifies the adiabatic functions. Because the hyperspherical adiabatic representation is a mathematically correct formulation of scattering theory, one gets the correct solutions on the circle at infinity. Thus the connection between Sturmian and adiabatic functions plays a critical role, even though exact solutions employ only one Sturmian function. For that reason it is valuable to identify just where the ZRP adiabatic functions agree with more realistic channel functions.

In the following section we compare the adiabatic potentials obtained in [23] for three identical bosons with those from the ZRP model. This comparison serves to locate regions where the ZRP model is applicable.

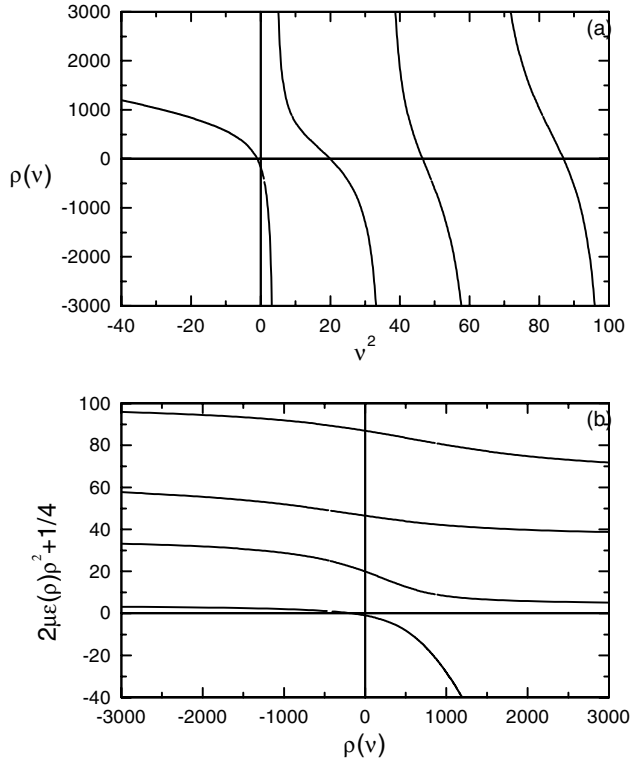

Figure 2. Plot of the pseudo-Sturmian eigenvalue $\rho(\nu)$. In (a) we plot $\rho(\nu)$ as a function of ν^2. In (b) the plot of (a) is rotated and flipped to give $2\mu\varepsilon(\rho)\rho^2 + \frac{1}{4}$ as a function of ρ.

3. Results and discussion

As mentioned in the introduction, ZRPs are used to model dilute Bose condensates and other cold systems. Bosons with different masses can be treated, but in this paper we consider three identical particles. We use the Sturmian method described in the previous section to compute adiabatic energy curves for three ^{4}He since accurate hyperspherical adiabatic calculations with realistic two-body potentials by Lee *et al* [23] are available. These authors take the mass of a ^{4}He atom as 7296.2994 au and compute an s-wave scattering length of 189.05 au. These parameters are used in our ZRP model.

Adiabatic eigenvalues for the symmetries $J^\pi = 0^+$, 1^+, 1^-, 2^+, 2^-, 3^+ and 3^-, where J is the total angular momentum and π is the parity, are reported in [23]. The ZRP model has two-body bound states only when the angular momenta l_{x_i} are equal to zero, as occurs for $\pi = (-1)^J$. The symmetry properties of these states are incorporated into the Sturmian functions defined by equation (8) and can be extracted using the behaviour of the hypergeometric functions and bispherical harmonics under coordinate inversion [14]. The states with $\pi = (-1)^{J+1}$ have $l_{x_i} > 0$ and integer values of ν in the ZRP model. They correspond to superpositions of degenerate hyperspherical harmonics with the same generalized angular momentum quantum number λ but different l_{x_i}, l_{y_i} and m, where $2m = \lambda - l_{x_i} - l_{y_i}$. For example, the 2^- eigenstate is a superposition of degenerate states with $\lambda = 5$, namely $l_{x_i} = 1$, $l_{y_i} = 2$, $m = 1$ and $l_{x_i} = 2$, $l_{y_i} = 3$, $m = 0$. Greater numbers of degenerate states are required for the eigenstates 1^+ and 3^+ and are not given here.

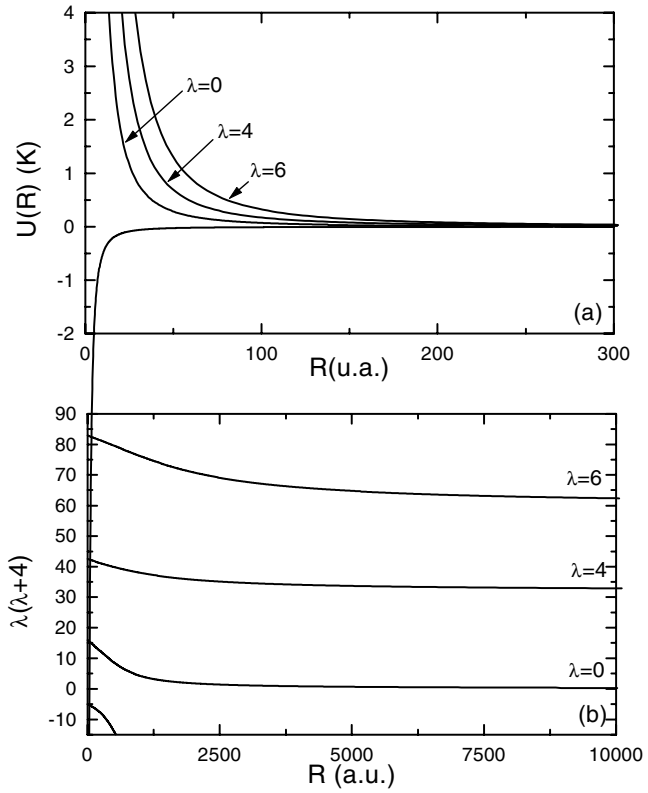

Figure 3. Adiabatic potential curves for the zero-range model of three helium atoms. In (a) energy eigenvalues $\varepsilon_n(R)$ corresponding to the bound and first three continuum states are shown. In (b) the same curves are transformed to show the approach of $\lambda(\lambda+4)$ to its asymptotic values. Atomic units are used for ρ and kelvin (K) for energy.

Adiabatic potential curves $\varepsilon(R)$ corresponding to the mentioned symmetries are shown in figure 4. The data points are from [23] and the full curves are the ZRP model equation (2) with (17). The agreement of the adiabatic potentials curve from [23] with equations (2) and (17) is good in general for $R > 50$ au. In contrast, expansions of the adiabatic potentials in powers of a/R require much larger values of R. The wider regions of agreement for the ZRP model include regions near $R \approx 2.5a$ which are known [5] to be important for three-body recombination.

To see more clearly the regions of agreement we plot $\lambda(\lambda+4)$ where λ relates to $\nu_n(R)$ according to $\nu_n(R) = \lambda + 2 = l_1 + l_2 + 2m + 2$. Figure 5 shows $\lambda(\lambda+4)$ as a function of R/a. We see that both calculations for the 0^+ state agree within 17% at $R/a \approx 0.25$. For smaller values of R, the actual shape of the two-body potentials becomes relevant. However, the hidden crossing theory [5] shows that recombination occurs near $R/a \approx 2.5$ since the bound and the first continuum adiabatic energy curves are degenerate at $R = (2.5918 + 2.9740\mathrm{i})a$. This implies that ZRP models include a significant part to the three-body dynamics of cold collisions. For example, collisions in the 100 nK range occur in Bose condensates. The lowest three-body potential has a value of 100 nK only for $R > 10^6$ au. At such large distances one needs an asymptotic representation of $\varepsilon(R)$. Such a representation is provided here by equation (2) with (17). This equation was given earlier for $J = 0$; here we have derived

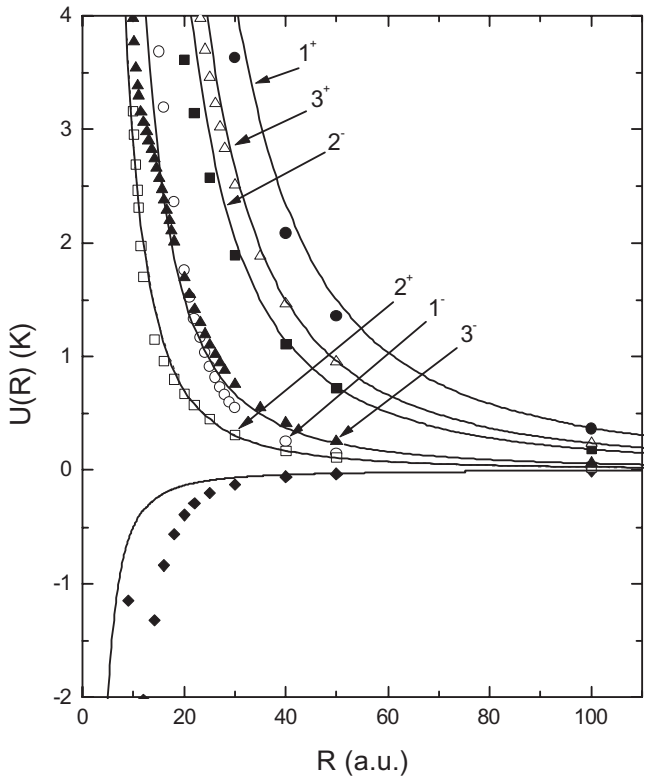

Figure 4. Adiabatic potential curves for three helium atoms. Energy eigenvalues $\varepsilon_n(R)$ corresponding to the states 0^+, 1^-, 1^+, 2^-, 2^+, 3^- and 3^+ are shown. Full curves are the ZRP model. The calculations of [23] are filled diamonds for 0^+, open and solid squares for 2^+ and 2^-, respectively, open and solid circles for 1^- and 1^+, respectively, and solid and open triangles for 3^- and 3^+, respectively.

the asymptotic form for arbitrary J. Note that for a total three-body energy of 100 nK the turning point on the lowest channel is at $R_T \approx 10^6$ au. Nonetheless, recombination occurs via tunnelling from this large R_T to $R \approx 500$ au. In this region our asymptotic result gives an accurate description of the three-body dynamics. It is important to note that cross sections also depend upon the potential curves in the inner region. This part contributes a phase that varies relatively slowly with the energy as in conventional MQDT theory.

For states $\pi = (-1)^{J+1}$ we compare the adiabatic energies from the calculations of Lee *et al* [23] with the ZRP model curves corresponding to asymptotic values of $\lambda = 8$, 6 and 4, for states 1^+, 2^- and 3^+ respectively. From figures 4 and 5 it is observed that our calculations depart from those of [23] for small values of R. The values of R for which the disagreement is notable increase with increasing λ. This probably relates to the high two-body kinetic energy for states with non-zero l_{x_i} and large $\nu(R)$. As the two-body kinetic energy increases with increasing $\nu(R)$ and decreasing R, smaller two-body distances are probed by the adiabatic eigenfunctions. At these smaller distances, two-body dynamics not included in the s-wave scattering lengths are expected to affect the adiabatic wavefunction, hence the departures from the ZRP model.

The 2^+ model curves and the computation of [23] agree within 1.9% for $R/a \approx 0.5$ ($R \approx 95$ au). On the other hand, at the same distance the 1^- and 3^- curves agree within

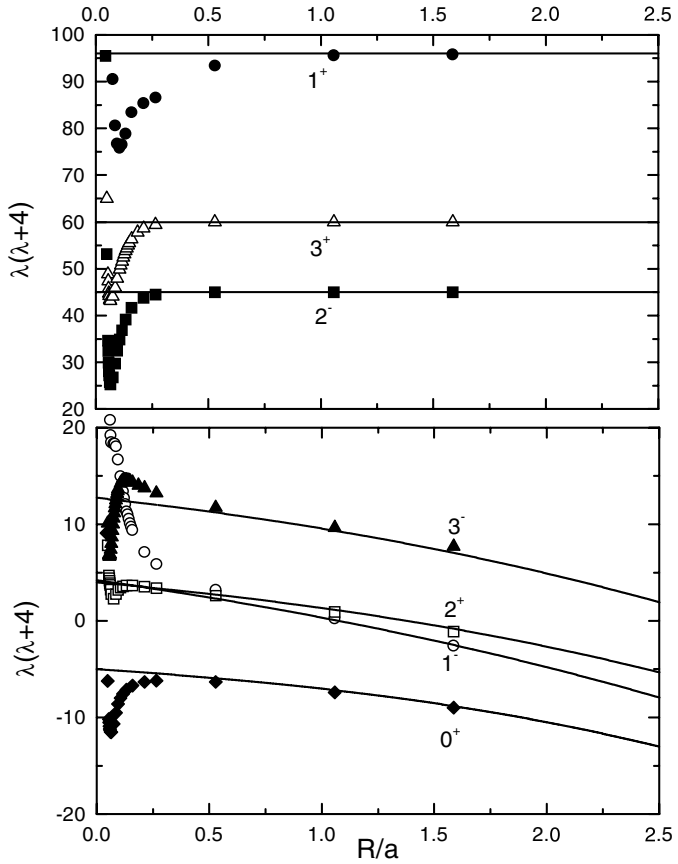

Figure 5. The adibatic eigenvalues $\lambda(\lambda+4)$ for 0^+, 1^-, 1^+, 2^-, 2^+, 3^- and 3^+ in the ZRP model are compared with the results of [23]. The symbols are as in figure 2.

13.3 and 3.4% respectively. Again, this is partially related to the high values of the two-body kinetic energy. We also note that for the 3^- eigenvalue near $R/a \approx 1.75$ the ZRP visually disagrees with the results of [23]. This is probably due to an inaccuracy in the last point of the data reported in [23], since the ZRP model should be accurate in this region.

The ZRP model results for the interaction of three ^{4}He bosons agrees in general terms with the adiabatic potentials of [23] in regions which are far from asymptotic in the parameter a/R. For $r_{0j} < R$, where r_{0j} is of the order of 100 au, the ZRP model is a good description of the system.

Exact solutions of the Schrödinger equation corresponding to three particles interacting via ZRPs include relevant parts of the three-particle dynamics. Usually asymptotic solutions are given by the tails of the potentials and no reactions occur in the asymptotic region. Expansions in powers of a/R correspond to these conventional asymptotic solutions. However, in the formulae presented here, the ZRP model describes a broad region that includes some of the main three-body dynamics. The ZRP results represent the first term in expansions in powers of r_{0j}/R and therefore describe real physical systems up to much smaller distances. In that sense the solutions of the ZRPs can be considered as good asymptotic wavefunctions for three particles interacting via short range two-body potentials. The exact ZRP solutions, if they

can be found in a convenient form, can then be used as asymptotic solutions in an R-matrix calculation over a surface S defined by $x_i = r_{0i}$. The advantage of such solutions derives from the smallness of r_{0i}/R thereby avoiding regions of large R where numerical calculations become difficult.

4. Conclusions

Hyperspherical adiabatic potential curves for the zero-range model have been compared with those from accurate numerical calculations for realistic two-body potentials. Analytic expressions for the adiabatic potential curves in the ZRP model and their relation to the Sturmian theory were discussed in section 2.

The adiabatic potential curves for three identical bosons in the ZRP model were presented in section 3. Eigenvalues obtained in [23] using realistic two-body potentials were compared with the ZRP model. We find that the ZRP model agrees well in general terms with the calculations of [23] for $R/a > 0.5$ for all the states considered. For that distance we found that the states $0^+$and 1^- agree within 17 and 13% respectively. For the states 1^+, 2^-, 2^+, 3^- and 3^+ the agreement is within 3% for $R/a \approx 0.5$ and greater. The states 1^+, 2^- and 3^+ are well described by hyperspherical harmonics for $R/a > 0.5$.

Acknowledgments

The authors thank Dr Brett Esry for kindly supplying us with the data from [23].

This research is sponsored by the Division of Chemical Sciences, Office of Basic Energy Sciences, US Department of Energy, under contract no DE-AC05-96OR22464 through a grant to Oak Ridge National Laboratory, which is managed by UT-Battelle, LLC under contract no DE-AC05-00OR22725. Support by the National Science Foundation under grant no PHY997206 is also gratefully acknowledged.

References

[1] Stenger J, Inouye S, Andrews M R, Miesner H J, Stamper-Kurn D M and Ketterle W 1999 *Phys. Rev. Lett.* **82** 2422
[2] Esry B D, Lin C D and Greene Ch H 1996 *Phys. Rev.* A **54** 394
[3] Schöllkopf W and Toennies J P 1996 *J. Chem. Phys.* **104** 1155
[4] Fedichev P O, Reynolds M W and Shlyapnikov G V 1996 *Phys. Rev. Lett.* **7** 2921
[5] Nielsen E and Macek J H 1999 *Phys. Rev. Lett.* **83** 1566
[6] Esry B D, Greene Ch H and Burke J P Jr 1999 *Phys. Rev. Lett.* **83** 1751
[7] Bedaque P F, Hammer H W and Van Kolck U 1999 *Nucl. Phys.* A **646** 444
Bedaque P F, Braaten E and Hammer H W 2000 *Phys. Rev. Lett.* **85** 908
[8] Esry B D, Greene C H, Zhou Y and Lin C D 1996 *J. Phys. B: At. Mol. Opt. Phys.* **29** L51
[9] Aymar M, Greene C H and Luc-Koening E 1996 *Rev. Mod. Phys.* **68** 1015
[10] Watanabe S 1982 *Phys. Rev.* A **25** 2074
[11] Zheng Zhen and Macek J 1988 *Phys. Rev.* A **38** 1193
[12] Denkov Yu N and Ostrovskii V N 1988 *Zero-Range Potentials and their Applications in Atomic Physics* (New York: Plenum)
[13] Gasaneo G, Ovchinnikov S Yu and Macek J H 2001 *J. Phys. A: Math. Gen.* **34** 8941
[14] Macek J H 1968 *J. Phys. B: At. Mol. Phys.* **1** 831
Lin C D 1995 *Rep. Prog. Phys.* **257** 1
[15] Macek J H *Few-Body Syst.* at press
[16] Nielsen E, Fedorov D V, Jensen A S and Garrido E 2001 *Phys. Rev.* **347** 373
[17] Kartavtsev O I and Macek J H *Few-Body Syst.* at press
[18] Nielsen E, Fedorov D V and Jensen A S 1998 *J. Phys. B: At. Mol. Opt. Phys.* **31** 4085

[19] Esry B D, Greene C H and Suno H 2002 *Phys. Rev.* A **65** 010705(R)
[20] Esry B D, Greene C G and Burke J P 1999 *Phys. Rev. Lett.* **83** 1751
[21] Macek J H, Ovchinnikov S Yu and Pasovets S V 1995 *Phys. Rev. Lett.* **74** 4631
[22] Kartavtsev O I 1999 *Few-Body Syst. Suppl.* **10** 199
[23] Lee T G, Esry B D, Gou B-C and Lin C D 2001 *J. Phys. B: At. Mol. Opt. Phys.* **34** L203
[24] Macek J H and Cavagnero M J 1996 *Phys. Rev.* A **58** 348
[25] Fano U and Lee C M 1973 *Phys. Rev. Lett.* **31** 1573
[26] Macek J H and Ovchinnikov S Yu 1996 *Phys. Rev.* A **54** 544
[27] Demkov Yu N 1968 *Proc. Invited Talks 5th Int. Conf. on the Physics of Electronic and Atomic Collisions (Leningrad, 1967)* ed I P Flaks and E S Solovyev (Boulder, CO: Joint Institute for Laboratory Astrophysics) p 186
[28] Morse P M and Feshbach H 1953 *Methods of Theoretical Physics* (New York: McGraw-Hill)
[29] Abramowitz M and Stegun I A 1970 *Handbook of Mathematical Functions* (New York: Dover)
[30] Gasaneo G, Ovchinnikov S Yu and Macek J H *Phys. Rev.* A at press
[31] Federov D V and Jensen A S 1993 *Phys. Rev. Lett.* **71** 4103
[32] Sadeghpour H R, Bohn J L, Cavagnero M J, Esry B D, Fabrikant I I, Macek J H and Rau A R P 2000 *J. Phys. B: At. Mol. Opt. Phys.* **33** R93